

Ultracompact Multimode Interference 3-dB Coupler with Strong Lateral Confinement by Deep Dry Etching

Yong Ma, Seoijin Park, Liwei Wang, and Seng Tiong Ho, *Member, IEEE*

Abstract—Extremely short InP–InGaAsP MMI 3-dB couplers ($L \sim 15\text{--}50 \mu\text{m}$) with conventional structure have been successfully fabricated. The significant size reduction was achieved by deep dry etching and tapered access waveguide with large S-bend design. Optical transmission measurements on these devices have been performed. An optical bandwidth about 80 nm with a limit of 2-dB excess loss was obtained for most of the couplers. During the whole tunable wavelength range ($\lambda \sim 1485\text{--}1580 \text{ nm}$), the imbalance is within $\pm 0.5 \text{ dB}$. Fabrication tolerance and polarization independence are also investigated and the results demonstrated the applicability of these ultracompact devices in high-density photonic integrated circuit.

Index Terms—3-dB coupler, deep dry etching, excess loss, imbalance, InP–InGaAsP, multimode interference, splitting ratio.

I. INTRODUCTION

RECENTLY, the design and fabrication of ultracompact multimode interference (MMI) devices have gained more and more interests because of their importance in photonic integrated circuit (PIC). MMI devices can function as power splitters or combiners [1], 3-dB couplers [2], and dual-channel wavelength multiplexers [3]. Probably, the most important MMI device is 3-dB coupler. To the best of our knowledge, the previously reported smallest MMI 3-dB coupler with conventional structure to date has a device length of $107 \mu\text{m}$ [2]. It seems more and more difficult to reduce the device size further with the conventional structure. The main problem is that direct coupling between the two access waveguides may happen when they get closer. Recently, a new design scheme has been proposed to avoid this problem by using a parabolically or linearly tapered MMI region instead of straight waveguide [4], [5]. The tapered MMI region basically has a smaller effective width than that of straight waveguide, which in turn makes the further reduction of device length possible. However, there are always tradeoffs. This new design is accompanied by the fabrication tolerance reduction, more power loss and larger power imbalance compared with the conventional one [5].

On the other hand, deep dry etching and tapered access waveguide with large S-bends give us an opportunity to reduce the device sizes without special MMI region design. In addition, deep etched waveguide can produce very strong lateral confinement which ensures a sufficient number of guided modes supported in

TABLE I
THE CALCULATED LENGTHS OF MMI 3-dB
COUPLERS FOR BOTH TE AND TM CASES

(W_{AG}, W_{MMI})		$(0.4 \mu\text{m}, 2.0 \mu\text{m})$	$(0.6 \mu\text{m}, 3.2 \mu\text{m})$	$(0.8 \mu\text{m}, 3.2 \mu\text{m})$
Length of MMI $L(\mu\text{m})$	TE	19.67	42.43	48.23
	TM	17.15	38.75	48.04

the MMI region to image the input field accurately. Therefore, deep etched waveguide can help to improve the image quality as pointed out in [2], [6], [7]. This benefit will become more significant in very short MMI devices as the number of modes is decreased by miniaturizing the device length. In this paper, we report our design, fabrication and measurement of ultracompact InP–InGaAsP MMI 3-dB couplers based on conventional structures. The devices are made by deep dry etching technique with device length ranging from 50 to $15 \mu\text{m}$. We believe that these devices are the smallest MMI 3-dB couplers made to date.

II. DESIGN AND FABRICATION

The 3-dB couplers were fabricated in a multilayer InP–InGaAsP wafer with a $0.65\text{-}\mu\text{m}$ -thick InGaAsP guiding layer ($\lambda_{\text{gap}} = 1.3 \mu\text{m}$). The access waveguide widths W_{AG} are $2 \mu\text{m}$ and tapered down to 0.4 , 0.6 , and $0.8 \mu\text{m}$ right before the S-bends leading to the MMI region. The S-bend has a radius of $20 \mu\text{m}$ to ensure the bending-loss to be negligible. The tapered section of the access waveguide has a length of $100 \mu\text{m}$ in order to avoid sharp mode transition. Such small tapered access waveguides make it possible to decrease the width of the MMI couplers further and, therefore, shrink the length significantly even in a conventional structure. Corresponding to the 0.4 , 0.6 , and $0.8\text{-}\mu\text{m}$ -wide access waveguides, the widths of the MMI devices W_{MMI} are 2 , 3 , $3.2 \mu\text{m}$. To facilitate our discussion, we just call them MMI1, MMI2, and MMI3. The lengths of the MMI region L were calculated based on the theory given in [6]. The results have been listed in Table I. From Table I, we can see that the longest is $48.23 \mu\text{m}$ and the shortest $17.15 \mu\text{m}$ and there is a small difference between TE and TM cases. To compensate the possible fabrication errors, device length variations of about $10 \mu\text{m}$ have been included in the pattern design. The wafer was then patterned through a mask of 250-nm thick 4% polymethylmethacrylate (PMMA) using electron-beam lithography. Optimized inductively coupled plasma (ICP) dry etching utilizing $\text{Cl}_2 : \text{Ar} (2 : 3)$ were employed to transfer the pattern onto the wafer with a 400-nm -thick SiO_2 as the etching mask at $250 \text{ }^\circ\text{C}$. The etching depth in this case is about $3 \mu\text{m}$. This deep etching technique is to provide very strong lateral

Manuscript received November 22, 1999; revised January 31, 2000. This work was supported by DARPA/AFOSR Program under Award F49620-96-0262/P005 and made use of MRSEC Control Facilities of Northwestern University supported by the NSF under Award DMR-9632472.

The authors are with the Department of Electrical and Computer Engineering, The Technological Institute, Northwestern University, Evanston, IL 60208 USA.

Publisher Item Identifier S 1041-1135(00)03589-8.

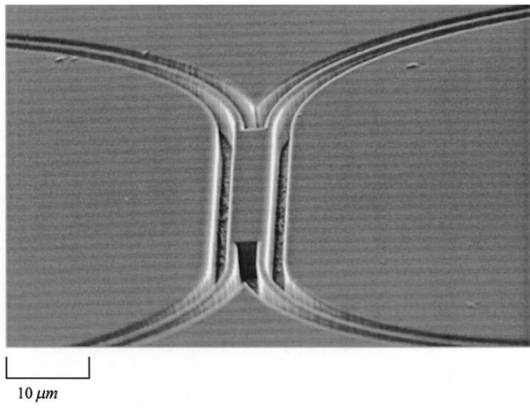


Fig. 1. Scanning electron micrograph of a MMI 3-dB coupler with $W_{AG} = 0.4 \mu\text{m}$ and $L = 20.5 \mu\text{m}$.

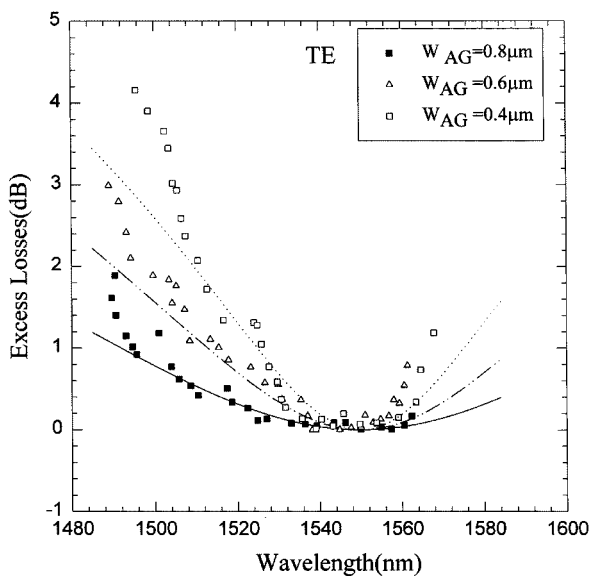


Fig. 2. Measured excess losses of MMI 3-dB couplers for the TE case. Lines are simulated results. Solid line: $W_{AG} = 0.8 \mu\text{m}$, $L = 49.0 \mu\text{m}$. Dashed line: $W_{AG} = 0.6 \mu\text{m}$, $L = 43.5 \mu\text{m}$. Dotted line: $W_{AG} = 0.4 \mu\text{m}$, $L = 20.0 \mu\text{m}$.

mode confinement so that no direct coupling happens between the access waveguides, which in turn helps to reduce the size of the MMI device and ensure a good image quality. A scanning electron microscope image of a MMI1 device is shown in Fig. 1.

III. RESULTS AND DISCUSSION

To study our MMI devices' spectral response end-fire coupling setup was used to measure the transmission output of the MMI couplers. We have plotted the excess-loss which is defined by the following as a function of wavelength in Fig. 2 for the TE case. The excess loss $\alpha = -10 \log((P_{\text{bar}} + P_{\text{cross}})/P_{\text{opt}})$, where P_{bar} , P_{cross} are the bar and cross power outputs and P_{opt} is the total power output at optimum wavelength which is $1.55 \mu\text{m}$ in our case. Measurement results show that the excess loss increases as the MMI device sizes shrink. From Fig. 2, we can see that an optical bandwidth about 80 nm can be achieved with

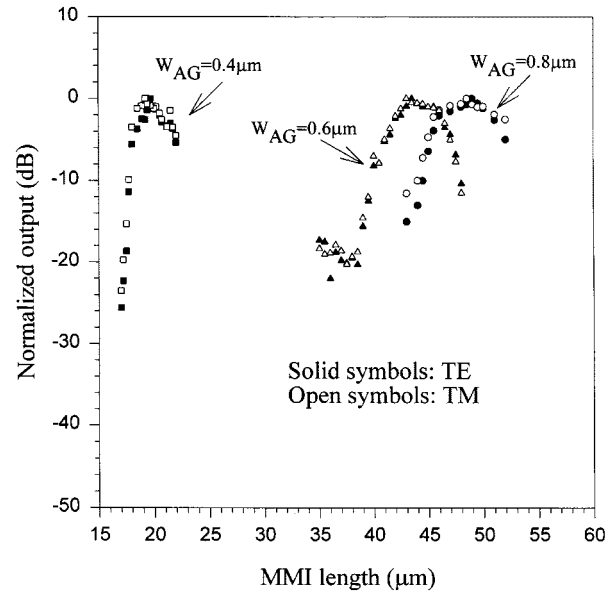


Fig. 3. Normalized output power $P = 10 \log((P_{\text{bar}} + P_{\text{cross}})/(P_{\text{bar}} + P_{\text{cross}})_{\text{opt}})$ as the function of MMI length of 3-dB couplers for both TE and TM cases at $\lambda = 1.55 \mu\text{m}$. Squares: $W_{AG} = 0.4 \mu\text{m}$. Triangles: $W_{AG} = 0.6 \mu\text{m}$. Circles: $W_{AG} = 0.8 \mu\text{m}$. Solid symbols: TE Open symbols: TM.

a limit of 1, 2, 4 dB excess losses for MMI3, MMI2, and MMI1. The device lengths for the three MMI's are 49.0, 43.5, and 20.0 μm which are very close to the calculated results. The higher excess losses associated with the smaller devices are due to the significantly increased scattering loss which is confirmed by our loss measurements on reference waveguides. No experimental data available for large S-bend at the moment as we did not put it in the design. However, we estimate the additional bending-loss brought by the S-bend should be less than 0.05 dB because of the strong lateral index difference (3.32:1.0) and large bend radius (20 μm). Note that the taper losses seem to be much higher than that given in [2]. It is probably due to 1) our etching depth is much deeper ($\sim 3.0 \mu\text{m}$); 2) our tapers are much narrower. Simulated results based on the approximation given in [8] are also plotted out as solid lines in Fig. 2. From Fig. 2, we also see a large discrepancy between our experimental data and the simulated results at short wavelength region. As pointed out in [8], index dispersion and material absorption may be responsible. To investigate how the MMI length affects the performance, we have plotted out the normalized output power [$P = 10 \log((P_{\text{bar}} + P_{\text{cross}})/(P_{\text{bar}} + P_{\text{cross}})_{\text{opt}})$ in dB, where $(P_{\text{bar}} + P_{\text{cross}})_{\text{opt}}$ is the total output power from the MMI with optimum length.] as a function of MMI length at $\lambda = 1.55 \mu\text{m}$ in Fig. 3. From Fig. 3 we can see that the excess loss due to length variation increases as the MMI length deviates away from the optimum values. This situation becomes severe as the access waveguide width decreases. Furthermore, these small MMI devices are weakly polarization dependent. The optimum length values of MMI3 are 49.0 μm for TE and about 48.5 μm for TM. From Fig. 3, we can see that the excess loss difference between TE and TM is less than 1 dB for most of the device lengths. Note that MMI2 and MMI1 have very similar results as MMI3 except that the length dependence is much more sharper and more losses are expected in those devices. Another important

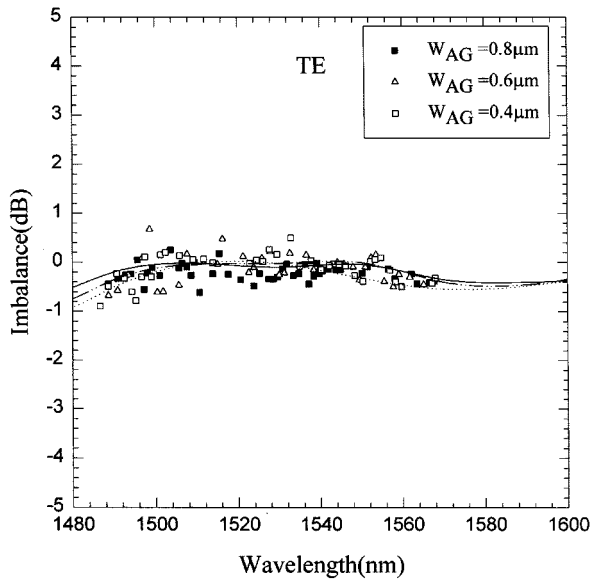


Fig. 4. Measured imbalance of MMI 3-dB couplers with optimum lengths for TE case. Lines are BPM simulated results. Solid line: $W_{AG} = 0.8 \mu\text{m}$, $L = 49.0 \mu\text{m}$. Dashed line: $W_{AG} = 0.6 \mu\text{m}$, $L = 43.5 \mu\text{m}$. Dotted line: $W_{AG} = 0.4 \mu\text{m}$, $L = 20.0 \mu\text{m}$.

parameter of 3-dB couplers is the power imbalance which is defined as $10 \log(P_{\text{bar}}/P_{\text{cross}})$ and describes the power difference between the two output waveguides. Fig. 4 presents the measured imbalance of these MMI devices with optimum lengths discussed above at different wavelengths for TE case. In Fig. 4, most of the measured data are within ± 0.5 dB during the tunable wavelength range. These data also agree with the beam propagation method (BPM) simulation (represented by the lines) qualitatively. Compared with TE, TM gives a little more imbalance which is less than 0.1 dB under same conditions. However, both cases show that the imbalance stays within ± 0.5 dB over the entire tunable wavelength range. With a power imbalance of ± 0.5 dB, the fabrication tolerance of the device length δL is about $8 \mu\text{m}$ for both MMI3 and MMI2, and $2 \mu\text{m}$ for MMI1. And the width tolerance δW is estimated to be about $0.26 \mu\text{m}$ for MMI3 and MMI2, $0.1 \mu\text{m}$ for MMI1.

IV. SUMMARY

MMI 3-dB couplers with extremely short lengths ($L \sim 15\text{--}50 \mu\text{m}$) in conventional structure have been fabricated and measured. Strong lateral confinement achieved using deep dry etching and the use of tapered access waveguide with large S-bends allow to shrink the device size significantly. Our devices are much shorter than the previously reported smallest MMI 3-dB coupler with conventional structure ($L \sim 107 \mu\text{m}$) and with tapered structure ($L \sim 66 \mu\text{m}$). Although there are more excess losses as expected, an 80-nm optical bandwidth with a limit of 2-dB excess loss is still available for the relatively longer devices. As power splitting, imbalance of less than ± 0.5 dB is obtained over the entire tunable wavelength range for all of the couplers fabricated. Such small devices show very weak polarization dependence in terms of output power and power imbalance. The fabrication tolerances are also comparable to previously reported results.

REFERENCES

- [1] J. M. Heaton, R. M. Jenkins, D. R. Wight, J. T. Parker, J. C. H. Birbeck, and K. P. Hilton, "Novel 1-to- N way integrated optical beam splitters using symmetric mode mixing in GaAs/AlGaAs multimode waveguides," *Appl. Phys. Lett.*, vol. 61, pp. 1754–1756, 1992.
- [2] L. H. Spiekman, Y. S. Oei, E. G. Metaal, F. H. Groen, I. Moerman, and M. K. Smit, "Extremely small multimode Interference couplers and ultrashort bends on InP by deep etching," *IEEE Photon. Technol. Lett.*, vol. 6, pp. 1008–1010, 1994.
- [3] M. R. Paiam, C. F. Janz, R. I. MacDonald, and J. N. Broughton, "Compact planar 980/1550-nm wavelength multi/demultiplexer based on multimode interference," *IEEE Photon. Technol. Lett.*, vol. 7, pp. 1180–1182, 1995.
- [4] D. S. Levy, R. Scarmozzino, Y. M. Li, and R. M. Osgood, Jr., "A new design for ultracompact multimode interference-based 2×2 couplers," *IEEE Photon. Technol. Lett.*, vol. 10, pp. 96–98, 1998.
- [5] D. S. Levy, K. H. Park, R. Scarmozzino, R. M. Osgood, Jr., C. Dries, P. Studenkov, and S. Forrest, "Fabrication of ultracompact 3-dB 2×2 MMI power splitters," *IEEE Photon. Technol. Lett.*, vol. 11, pp. 1009–1011, 1999.
- [6] L. B. Soldano and E. C. M. Pennings, "Optical multimode interference devices based on self-imaging: Principles and applications," *J. Lightwave Technol.*, vol. 13, pp. 615–627, 1995.
- [7] R. Ulrich and T. Kamiya, "Resolution of self-images in planar optical waveguides," *J. Opt. Soc. Amer.*, vol. 68, pp. 583–592, 1978.
- [8] P. A. Besse, M. Bachmann, H. Melchior, L. B. Soldano, and M. K. Smit, "Optical bandwidth and fabrication tolerance of multimode interference couplers," *J. Lightwave Technol.*, vol. 12, pp. 1004–1009, 1994.